

MiR-944/CISH mediated inflammation via STAT3 is involved in oral cancer malignance by cigarette smoking

Hsuan-Yu Peng^a; Jenn-Ren Hsiao^b; Sung-Tau Chou^a; Yuan-Ming Hsu^a; Guan-Hsun Wu^a; Yi-Shing Shieh^c; Shine-Gwo Shiah^{a,d,e,*}

^aNational Institute of Cancer Research, National Health Research Institutes, Miaoli 35053, Taiwan; ^bDepartment of Otolaryngology, Head and Neck Collaborative Oncology Group, National Cheng Kung University Hospital, College of Medicine, National Cheng Kung University, Tainan 70101, Taiwan; ^cDepartment of Dentistry, Tri-Service General Hospital, National Defense Medical Center, Taipei 11490, Taiwan; ^dCancer Center, Wan Fang Hospital, Taipei Medical University, Taipei 11696, Taiwan; ^ePh.D. Program in Environmental and Occupational Medicine, Kaohsiung Medical University, Kaohsiung 80708, Taiwan

Abstract

The cytokine-inducible Src homology 2-containing protein (CISH) is an endogenous suppressors of signal transduction and activator of transcription (STAT) and acts as a key negative regulator of inflammatory cytokine responses. Downregulation of CISH has been reported to associate with increased activation of STAT and enhanced inflammatory pathways. However, whether microRNAs (miRNAs) play a crucial role in CISH/STAT regulation in oral squamous cell carcinoma (OSCC) remains unknown. The expression of CISH on OSCC patients was determine by quantitative real-time PCR (qRT-PCR) and immunohistochemistry. Specific targeting by miRNAs was determined by software prediction, luciferase reporter assay, and correlation with target protein expression. The functions of miR-944 and CISH were accessed by transwell migration and invasion analyses using gain- and loss-of-function approaches. Enzyme-linked immunosorbent assay (ELISA) and qRT-PCR were used to evaluate the pro-inflammation cytokines expression under the miR-944, CISH, NNK or combinations treatment. We found that the CISH protein, which modulates STAT3 activity, as a direct target of miR-944. CISH protein was significantly down-regulated in OSCC patients and cell lines and its level was inversely correlated with miR-944 expression. The miR-944-induced STAT3 phosphorylation, pro-inflammation cytokines secretion, migration and invasion were abolished by CISH restoration, suggesting that the oncogenic activity of miR-944 is CISH dependent. Furthermore, tobacco extract (NNK) may contribute to miR-944 induction and STAT3 activation. Antagomir-mediated inactivation of miR-944 prevented the NNK-induced STAT3 phosphorylation and pro-inflammation cytokines secretion. Altogether, these data demonstrate that NNK-induced miR944 expression plays an important role in CISH/STAT3-mediated inflammatory response and activation of tumor malignancy.

Neoplasia (2020) xx xxx–xxx

Abbreviations: 3'-UTR, 3'-untranslated region, BNIP3, BCL2 interacting protein 3, CCL3, chemokine (C–C motif) ligand 3, CCL5, chemokine (C–C motif) ligand 5, CCR5, C–C chemokine receptor type 5, COX-2, Cyclooxygenase 2, EMT, epithelial-to-mesenchymal transition, GAPDH, Glyceraldehyde 3-phosphate dehydrogenase, GATA6, GATA binding protein 6, HECW2, HECT domain ligase W2, IL-1 β , interleukin-1 β , IL-2, interleukin 2, Inos, Inducible nitric oxide synthase, MDSCs, myeloid-derived suppressor cells, miRNA, microRNA, OSCC, Oral squamous cell carcinoma, PGE2, prostaglandin E2, qRT-PCR, Quantitative real-time polymerase chain reaction, S100PBP, S100P binding protein, SH2, Src homology, SOCS, Suppressors of cytokine signaling, STAT, signal transducer and activator of transcription, TAM, tumor-associated macrophage, VEGF-A, vascular endothelial growth factor-A

* Corresponding author: National Institute of Cancer Research, National Health Research Institutes, No. 35, Keyan Road, Zhunan City, Miaoli 35053, Taiwan.

e-mail addresses: hsiaojr@mail.ncku.edu.tw (J.-R. Hsiao), 080828@nhri.edu.tw (S.-T. Chou), 080828@nhri.edu.tw (Y.-M. Chou), 080828@nhri.edu.tw (Y.-M. Chou), 080828@nhri.edu.tw (Y.-M. Chou), 080828@nhri.edu.tw (Y.-M. Chou), 980406@nhri.edu.tw (Y.-M. Hsu), ndmcyss@mail.ndmctsg.edu.tw (Y.-S. Shieh), davidsg@nhri.edu.tw (S.-G. Shiah).

Keywords: CISH, STAT3, microRNA, miR-944, Inflammation, Oral cancer

Introduction

Head and neck squamous cell carcinoma is one of leading cause of cancer deaths, and oral squamous cell carcinoma (OSCC) accounted for about 90% of head and neck cancer [1]. Despite chemotherapy and radiotherapy were frequently adopted as a component of the postoperative intensive therapy with the aim of the reducing recurrence rates and the probability of metastasis [2,3]. However, thus far, no effective measures have been available to reduce the loco-regional recurrences and lymph node metastasis in OSCC patients [4]. Thus, better approaches for the treatment of OSCC will eventually require a better understanding of the molecular mechanisms that initiate and drive cancer malignant progression.

Recently, the importance of inflammation in tumor initiation and malignant progression has been extensively investigated [5], including malignant cell transformation, metastasis and generating an inflammatory microenvironment that further facilitates tumor progression [6]. This process is required by the presence of inflammatory cells and inflammatory mediators, consisting primarily of cytokines and chemokines [7]. For example, tumor necrosis factor- α (TNF- α) and interleukin (IL) family (such as IL-6, IL-1 β , IL-17 and IL-23), which support tumor growth, angiogenesis, invasion and metastasis, and maintain a cancer-promoting inflammatory environment [7–10]. A main common feature of these cytokines that are positively regulated by signal transducer and activator of transcription (STAT) family proteins, especially STAT3 [6]. STAT3 signaling is a major pathway for cancer inflammation because it is frequently aberrant and persistent activation in cancer cells and capable of inducing a large number of genes that are crucial for facilitating a tumor promoting inflammatory microenvironment, both at the tumor initiation and during cancer progression [11,12]. Under normal condition, the activity of STAT proteins is tight regulation by the induction of suppressors of cytokine signaling (SOCS) proteins. SOCS proteins are negative feedback regulators of cytokine signaling mediated by the Janus kinase (JAK)-STAT signaling pathway [13]. The SOCS family consists of 8 members, including SOCS1–7 and cytokine-inducible SH2 containing protein (CISH), which silence the STAT pathways by competing binding to JAKs and inhibiting their kinase activities, by masking STAT binding sites of the cytokine receptor, or by targeting proteins for proteasomal degradation [14]. Aberrant regulation of SOCS family proteins has been linked to a variety of inflammatory diseases, including cancer [15,16]. Therefore, dysregulation of SOCS proteins could be one of the important mechanisms for constitutive STAT activation and cancer inflammation.

Silencing of SOCS proteins is frequently observed in various cancers [17]. Genetic dysregulation, including genomic deletion [18,19], mutation [20] and single nucleotide polymorphism [21,22], as well as epigenetic dysregulation, including DNA hypermethylation [23–25] and histone modification [26,27], have been often discussed to participate in SOCS genes silencing. Recently, increasing evidence also suggests that microRNAs (miRNAs) play important roles in the altered expression of a number of SOCS proteins in cancer cells [17]. MiRNAs are short non-coding RNAs that bind to complementary sequences on target mRNAs to induce gene silence either by inhibiting protein translation or by increasing degradation of the mRNA [28]. Previous studies have shown that miR-155 and miR-19a can downregulate the expression of SOCS1 by directly binding the 3'-UTR of the SOCS1 mRNA and enhances the phosphorylation of STAT3 [29–31]. Another study demonstrated that miR-194 and miR-424-5p significantly decrease SOCS2 expression and promote cancer migration and invasion [32,33]. Moreover, miR-221 and miR-203 have been reported to regulate proliferation, apoptosis, and chemosensitivity by targeting SOCS3 [34,35]. These observa-

tions strongly suggest that aberrant miRNAs expression, which target SOCS family proteins, may affect STAT pathway and play cancer-promoting effect.

Aside from miRNAs, epidemiological studies and experimental evidences suggest that many environmental factors, such as UV irradiation, chemical carcinogens and cigarette smoking, can increase phosphorylation of STAT3 and link to inflammation-associated tumorigenesis in several types of cancer, including oral cancer [36–40]. Although cigarette smoke can activate STAT3 activity during oral carcinogenesis and promote cell survival, proliferation, epithelial-mesenchymal transition and angiogenesis [36,41,42], however, the molecular mechanisms of STAT3 activation induced by cigarette smoke remain unclear. In this study, we demonstrated that the exposure of oral cancer cell lines to 4-(Methylnitrosamino)-1-(3-pyridyl)-1-butanone (NNK), one of the major components of tobacco, significantly induced miR-944 expression. Up-regulation of miR-944 directly targeted CISH, a member of SOCS family proteins, and increased the STAT3 phosphorylation, which is crucial for the expression of genes encoding pro-inflammatory mediators, such as chemokine (C-C motif) ligand 3 (CCL3), CCL5, interleukin-1 β (IL-1 β), cyclooxygenase 2 (COX-2) and inducible nitric oxide synthase (iNOS). Thus, these findings defined a link between cigarette smoke and inflammation processes suggested a novel role of miR-944 in stimulating STAT3 activity through suppression of CISH protein, implicating an additional therapeutic strategy may be helpful to overcome oral cancer in inflammatory condition.

Material and methods

Clinical samples

Primary tumour tissues and their adjacent non-tumorous epithelia from 33 patients harboring clinically localized oral cavity were received curative surgery from 1999 to 2010. The study protocol was approved by the Research Ethics Committee of National Health Research Institutes (EC1040409-E) and Institutional Human Experiment and Ethic Committee of National Cheng Kung University Hospital (HR-97–100) for the use of clinical materials for research purpose. Informed consent was obtained from each patient. Tissues were obtained before chemotherapy or radiation therapy and immediately snap-frozen in liquid nitrogen, then stored at -80°C before RNA extraction. Total RNA (including miRNA) was isolated using the miRNeasy Mini Kit (Qiagen, #217004) according to the manufacturer's protocol.

Cell lines and culture condition

OEC-M1 cells were cultured in RPMI 1640, Cal27 cells were maintained in DMEM and SAS cells were growth in DMEM/F12 (1:1). DOK cells were maintained in DMEM supplemented with 1 mM sodium pyruvate, FaDu cells were growth in α -MEM supplemented with 1 μM hydrocortisone. SCC-25, SCC-9 and SCC-4 cells were cultured in DMEM/F12 (1:1) supplemented with 0.5 mM sodium pyruvate and 1 μM hydrocortisone. All basal culture media (Gibco, Grand Island, NY, USA) were supplemented with 10% fetal bovine serum (FBS, Kibbutz BeitHaemek, Israel). Transformed oral keratinocytes (OKB4/hTERT) were obtained from ScienCell and cultured in Keratinocyte-SFM (Gibco, Grand Island, NY, USA) according to the manufacturer's instructions. All cells were maintained in a humidified incubator at 37°C in a 5% CO_2 atmosphere. NNK was purchased from Sigma-Aldrich

(St. Louis, MO) and dissolved in DMSO (Sigma-Aldrich) as 0.5 M stock solution. To assay the effects of NNK on OSCC cells, OE-CM1 and SCC-25 were short-term treated with NNK (10–40 μ M) or DMSO vehicle for 24, 48 or 72 h. For gene knockdown experiments, the lentiviral shRNA clones for CISH (shCISH) and non-targeting pLKO_TRC control plasmid (NS) were obtained from the National RNAi Core Facility (Academia Sinica, Taiwan). For transfection of shRNA plasmids, cells were transiently transfected with 2 μ g of plasmids using Lipofectamine 2000 from Invitrogen (CA, USA) according to the manufacturer's protocol.

Immunohistochemistry

CISH Protein expression was immunohistochemically examined using multiple head and neck cancer tissue array (# HN803b, US Biomax Inc., Rockville, MD). This multiple head and neck carcinoma tissue array contains 9 cases of normal tongue tissue, 22 cases of tongue squamous cell carcinoma and 47 cases of other subtype of head and neck carcinoma tissue (including larynx squamous cell carcinoma, nose squamous cell carcinoma and carcinoma sarcomatodes). We used 9 cases of normal tongue tissue and 22 cases of tongue squamous cell carcinoma to represent the oral cavity specimens. Briefly, sections were deparaffinized and rehydrated through graded alcohols. Antigen retrieved in heated citric acid buffer (pH 6.0) and endogenous peroxidase activity was blocked with 3% hydrogen peroxide for 10 min. After washing, Sections were blocked and then incubated with anti-human CISH polyclonal antibody (GTX100216, 1:100, GeneTexInc, Irvine, CA, USA) at 4 °C overnight. Specific signals were then developed with LSAB+kit (DakoCytomation, CA, USA) using diaminobenzidine (Biocare) as chromogen. Sections were then counterstained with hematoxylin and observed under light microscope. Tumor CISH level was scored according to CISH staining intensity as follows: no staining, weak, intermediate and strong. Two pathologists independently assessed all the scorings.

RNA extraction and quantitative Real-Time PCR (qRT-PCR)

Total RNA was extracted from OSCC cells using TRIzol reagent (Life Technologies, Gaithersburg, MD) according to the manufacturer's protocol. For mature miRNA detection, the cDNA was synthesized from total RNA using miRNA-specific primers in a Biometra T3000 thermocycler (Biometra GmbH, Germany) by following the manufacturer's instructions. The miRNA cDNA was quantified using TaqMan Universal PCR Master Mix (Applied Biosystems) and normalized with RNU44, serving as the internal control. For mRNA detection, the cDNA was synthesized using random hexamer primers and SuperScript III reverse transcriptase (Invitrogen, Carlsbad, CA) and then used as template to quantify CISH, CCL3, CCL5, IL-1 β , COX-2, iNOS and TP63 using gene-specific primers and normalized to the expression of GAPDH gene. The primer sequences were used for PCR reaction as followed: 5'-TTC GGG AAT CTG GCT GGT ATT-3' (forward) and 5'-GAA CGT GCC TTC TGG CAT CT-3' (reverse) for CISH expression, 5'-AGT TC TCT GCA TCA CTT GCT G-3' (forward) and 5'-CGG CTT CGC TTG GTT AGG AA-3' (reverse) for CCL3 expression, 5'-GAG TAT TTC TAC ACC AGT GGC AAG-3' (forward) and 5'-TCC CGA ACC CAT TTC TTC TCT-3' (reverse) for CCL5 expression, 5'-CCC TTG GGT GTC AAA GGT AA-3' (forward) and 5'-GCC CTC GCT TAT GAT CTG TC-3' (reverse) for COX-2 expression, 5'-ATG ATG GCT TAT TAC AGT GGC AA-3' (forward) and 5'-GTC GGA GAT TCG TAG CTG GA-3' (reverse) for IL-1 β expression, 5'-GCA GAA TGT GAC CAT CAT GG-3' (forward) and 5'-ACA ACC TTG GTG TTG AAG GC-3' (reverse) for iNOS expression, 5'-GAA GGT GAA GGT CGG AGT-3' (forward) and 5'-GAA GAT GGT GAT GGG ATT

TC-3' (reverse) for GAPDH expression. All qRT-PCR reactions were run on an Applied Biosystems StepOne Plus real-time PCR system. The expression level was defined based on the threshold cycle (Ct), and relative expression levels were calculated as $\Delta\Delta C_t$ after normalization with reference control.

Protein extraction and western blot analysis

Cells were lysed using protein extraction buffer (50 mM Tris-HCl, 1% NP-40, 150 mM NaCl, and 0.1% SDS) containing protease inhibitor cocktail (Sigma-Aldrich, Inc.) and phosphatase inhibitor (1 mM Na₃VO₄). Protein concentrations were then determined by the BCA assay kit (Thermo, USA) with bovine serum albumin as standard. Equivalent amounts of protein lysates were subjected to 10–12% SDS-PAGE gel and transferred to polyvinylidene fluoride membranes (Pall Life Sciences, Glen Cove, NY). The membranes were probed with specific antibodies against CISH (#8731, Cell signaling, Danvers, MA), STAT3 (#610189, BD Biosciences, NJ), phospho-STAT3 (p-STAT3, Tyr⁷⁰⁵) (#9131, Cell signaling), STAT5 (#25656, Cell signaling), phospho-STAT3 (p-STAT5, Tyr⁶⁹⁴) (#9359, Cell signaling), COX-2 (#12282, Cell signaling), and iNOS (ab204017, Abcam, Cambridge, MA). GAPDH (GTX100118, Thermo Fisher Scientific, San Jose, CA) was used as an internal control. Signals from HRP-coupled secondary antibodies were visualized by the enhanced chemiluminescence (ECL) detection system (PerkinElmer, Waltham, MA) and the chemiluminescence was exposed onto Kodak X-Omat film (Kodak, Chalon/Paris, France). Protein levels were determined as the integrated area (pixels) of the band intensities by densitometry analysis with Image J software (Bethesda, MD, USA). The numerical values for protein band intensities were corrected with the values of the GAPDH bands.

Plasmid construction

For gene expression, a 828-base pair fragment of CISH was amplified by PCR and cloned into the BamHI and EcoRI sites of the pcDNA3.1 plus vector (Invitrogen, Gaithersburg, MD), using the CISH cloning primers: 5'-GGG GAT CCA TGT ACC TAG AAC ACA CCA GCA-3' (forward) and 5'-GGG AAT TCT CAG A GC TGG AAG GGG TAC TGT C-3' (reverse). For miRNA luciferase reporter assay, the CISH 3'-UTR region was generated by subcloning PCR-amplified full-length human CISH cDNA (1170-base pair from the stop codon respectively) into the XhoI/XbaI sites of pmiRGLO firefly luciferase-expressing vector (Promega, WI, USA), using the cloning primers: 5'-GGG GGC TCG AGC TGT ACG GGC CAA TCT GCC CAC-3' (forward) and 5'-GGT CTA GAC ACA AC T GAA AAT CGG CCC CAT TGA G-3' (reverse). The miRNA binding sites mutation reporters were constructed by using Site-Directed Mutagenesis Kit (Stratagene, La Jolla, CA) with specific primers: 5'-ATG ATT TAA TGG TTA TAG CAA AGA ACA GTT TGG TGG TCT TT-3' (forward) and 5'-TGC TAT AAC CAT TAA ATC AT G AAG TCT TAT CAG ACG TGT ATT T-3' (reverse) for site.

Luciferase reporter assays

The STAT3 reporter plasmid (pm67-tk-Luc) was kindly provided from Dr. Wu-Chou Su [43]. Briefly, to construct pm67-tk-Luc plasmid, an oligonucleotide containing four copies of the sequence GGTTCCCGTAAATGCATCA (TTCCCGTAA is the STAT-binding site) was introduced in the AccI-BamHI sites of pTATA-tk-Luc upstream of the minimal promoter. Cells were harvested 48 h after co-transfection of pm67-Luc reporter vector with control vector (Vec) or CISH expression vector (CISH) with Dual Luciferase Assay System (Promega, USA) according to the manufacturer's protocol. For 3'-UTR reporter assay, cells were cultured in 24-well plates and co-transfected with 300 ng of CISH

3'-untranslated region (UTR) wild type or mutant type pmirGLO reporter plasmid and with 25 nM of miR-944 mimics (PM) (Applied Biosystems, Carlsbad, CA) or control oligonucleotide (NC) (Applied Biosystems) with Lipofectamine 2000 according to the manufacturer's instructions. The luciferase assay was performed 48 h post transfection with Dual Luciferase Reporter Assay System (Promega, USA) as described by the manufacturer's protocol. Luminometry readings were obtained using an Orion L luminometer (Berthold).

Enzyme-linked immunosorbent assay (ELISA)

Transfected and control OEC-M1 and SCC-25 cells were seeded onto 6-well plates at 2×10^6 cells in serum-free culture medium. After culture for total 48 h, the supernatant was collected and purified by passing through 0.2 μm polyethersulfone membrane (Corning Costar, Rochester, NY, USA) respectively to remove cell debris for cytokines assay by ELISA. The cytokines in culture supernatant, including CCL3, CCL5, and IL-1 β , were quantified using Ready-to-use ELISA Kits (PeproTech, International, Inc., NJ, USA) according to the manufacturer's protocol.

Cell viability assay

Transfected SAS and SCC-4 cells were seeded into 96-well plates (3000 cells/well). After overnight incubation, 200 μl of culture medium was dispensed into each well. Following 72-h treatment, 3-[4,5-dimethyl thiazol-2-yl]-2,5-diphenyl tetrazolium bromide (MTT) dye (Calbiochem, CA, USA) was added. After 2 h of incubation, the medium and MTT dye were removed by slow aspiration and 100 μl of dimethyl sulfoxide (DMSO) was added to dissolve the remaining MTT formazan crystals. The absorbance at 550 nm was measured using a 96-well plate SpectraMax 250 reader (Molecular Devices, CA, USA).

Cell migration and invasion assay

The migration and invasion assays were performed using 24-well Fluoro-Blok insert-based assays system (8 μm pore size membrane; BD Biosciences, Franklin Lakes, NJ). The culture insert was coated to a density of 40 $\mu\text{g}/\text{insert}$ of Matrigel Basement Membrane Matrix (BD Biosciences) for invasion assay, but was coated nothing for migration assay. Subsequently, 5×10^4 cells were seeded in the upper chamber in culture medium containing 10% NuSerum. After incubating 24 h for invasion assay and 12 h for migration assay at 37 $^{\circ}\text{C}$, the cells that passed through the Fluoro-Blok membrane were fixed with 95% methanol and stained with propidium iodide. The fluorescence images were then counted with Analytical Imaging Station software package (Imaging Research, Ontario, Canada).

Statistical analysis

Paired t-tests were performed to compare the CISH mRNA intensity and expression level in cancer tissues and the corresponding adjacent non-tumorous epithelia. Experimental graphs are expressed as the mean \pm standard error (SE) from at least three independent experiments. Linear correlation and Pearson correlations were used to evaluate the correlation between 2 variants. Differences with the various treatment groups were assessed using the Student's t-test or one-way analysis of variance (ANOVA) analysis with multiple comparisons in cases in which more than 2 conditions were compared on the same set. Calculations were performed using Graph Pad Prism Ver. 4.01 (San Diego, CA). A *p*-value <0.05 was considered as significant.

Results

Down-regulation of CISH in OSCC tissues and cell lines

In order to identify dysregulated genes in oral cancer, we have performed microarray analysis from 40 of OSCC specimens and uploaded the data to Gene Expression Omnibus (GEO) under accession number GSE37991. From the microarray data, we found that CISH levels were significantly downregulated in tumors compared with their corresponding normal samples using microarray data generated from 40 pairs of OSCC specimens ($P < 0.001$, Fig. 1A, B). CISH expression levels were then validated in another 33 of OSCC tissue sample (Supplementary Table S1), using quantitative RT-PCR, and were found to be significantly downregulated in tumors ($P < 0.001$, Fig. 1C, left), but there was no significant difference in CISH expression levels in stage I-II vs stage II-IV patients (Fig. 1C, right). To confirm this trend in protein level, we used CISH-specific antibody for immunohistochemistry in normal tissue and OSCC biopsies from individual cases tissue array. We found that CISH protein level were high in 88.9% of normal samples (staining intensity: No staining = 0%, Weak = 11.1%, Intermediate = 22.2%, Strong = 66.7%), whereas only 27.3% showed a high stain signal in tumor samples (staining intensity: No staining = 31.8%, Weak = 40.9%, Intermediate = 18.2%, Strong = 9.1%) (Fig. 1D). Consistent with this, our western blotting analysis revealed that CISH levels are relatively lower in the most of OSCC cell lines when compared with the transformed normal human keratinocyte (Fig. 1E).

CISH mediates cellular functions through STAT3 inhibition

To evaluate the biological functions of CISH during the progression of OSCC, We ectopically expressed CISH in SAS and SCC-4 cells, which exhibit low levels of endogenous CISH protein. The results showed that CISH mRNA was significantly elevated in SAS and SCC-4 cells (Fig. S1A), and the expression of CISH strongly reduced STAT3 phosphorylation (Fig. 2A) and its transcriptional activity (Fig. 2B). Instead, we silenced CISH in OEC-M1 and SCC-25 cells, which exhibit high levels of endogenous CISH protein, using CISH-specific lentiviral shRNA construct (shCISH) and found that shRNA-mediated silencing of ectopic CISH increased STAT3 phosphorylation (Fig. S1B). These results indicate that STAT3 activity is primarily subject to negative regulation by CISH in OSCC cells. Next, the phenotypic impact of CISH overexpression was tested in SAS and SCC-4 cells. The MTT assay showed that CISH overexpression has no significant change on cell growth (Fig. S1C). However, we observed a significant decrease in the migration and invasion of SAS and SCC-4 cells with CISH overexpression (Fig. 2C, D). In addition, STAT3 activation is recognized as an important link between inflammation and cancer [6,44]. We then hypothesized that CISH might inhibit STAT3-mediated downstream pro-inflammation molecules secretion in OSCC cells. We found that the CISH overexpression was associated with decreased STAT3-mediated pro-inflammation cytokines expression, including CCL3, CCL5, IL-1 β , COX-2 and iNOS, both at mRNA (Fig. S1D) and protein level (Fig. 2E, F).

CISH is a direct target of miR-944

Next, we attempted to investigate whether miRNA plays a major role in CISH downexpression in OSCC. To determine the possible mechanism for CISH dysregulation, we surveyed the configuration of miRNA-binding sites within the 3'-untranslated region (3'UTR) of CISH mRNA. We used targeting algorithms (TargetScan and microRNA.org) combined with OSCC patients' miRNA microarray data (GSE45238) [45] to search for putative miRNAs that might bind to CISH mRNA

(Fig. 3A). Bioinformatics analysis identified three miRNAs, miR-7, miR-944 and miR-135b, which could potentially binding in the 3'-UTR of CISH mRNA. However, only miR-7 and miR-944 were markedly up-regulated in OSCC tissues compared with that in paired adjacent nontumor tissues (Fig. S2). We next evaluated protein expression level of CISH in miR-7 and miR-944 overexpression (PM) cells. The results showed that the CISH expression was dramatically suppressed in miR-944-overexpressing cells, not in miR-7-overexpressing cells, compared with that in control cells (NC) (Fig. 3B). To further confirm whether miR-944 could directly target CISH, we constructed and cloned the CISH 3'-UTR fragment containing the putative miR-944 binding sites (wild-type and mutant) into the pmirGLO reporter plasmid (Fig. 3C). We then performed luciferase reporter assay in OEC-M1 and SCC-25 cells. Luciferase assays showed that the expression of the wild-type, but not the mutant plasmid, was suppressed in miR-944-overexpressing cells (Fig. 3D). We next analyzed another OSCC testing cohort using qRT-PCR approach and found a significant inverse correlation between the expression levels of CISH and miR-944 ($r = -0.35$, $p = 0.04$) (Fig. 3E). Furthermore, transfection of miR-944 mimics in OEC-M1 and SCC-25 cells not only decreased CISH protein expressions but also increased STAT3 phosphorylation in a dose-dependent manner (Fig. 3F). By con-

trast, transfection of miR-944 inhibitors (AM) increased CISH protein in OEC-M1 and SCC-25 cells and decreased STAT3 protein phosphorylation (Fig. 3G). Taken together, our results showed that CISH is a direct target of miR-944. Overexpression of miR-944 in OSCC cells decreases CISH protein and increases STAT3 activity, suggesting an interaction between miR-944/CISH/STAT3 signaling pathways.

MiR-944 regulates cellular functions through direct binding of CISH

To further confirm that miR-944 mediate the downregulation of CISH to promote tumorigenicity. For this purpose, we constructed a vector-based CISH expression plasmid lacking 3'-UTR sequence, and thus the CISH mRNA is not targeted by miR-944. Cells transfected with CISH plasmid without 3'-UTR were able to reduce STAT3 phosphorylation in the presence of miR-944 mimics (PM) (Fig. 4A). Moreover, CISH restoration was able to reduce the miR-944-induced pro-inflammation molecules expression (such as COX-2 and iNOS) (Fig. 4B and Fig. S3A) and pro-inflammation cytokines secretion (such as CCL3, CCL5 and IL-1 β) (Fig. 4C). We further assessed the effect of CISH on the in vitro migration and invasion potential of OEC-M1 cells by transwell assay. As expected, the restoration of CISH potently suppressed

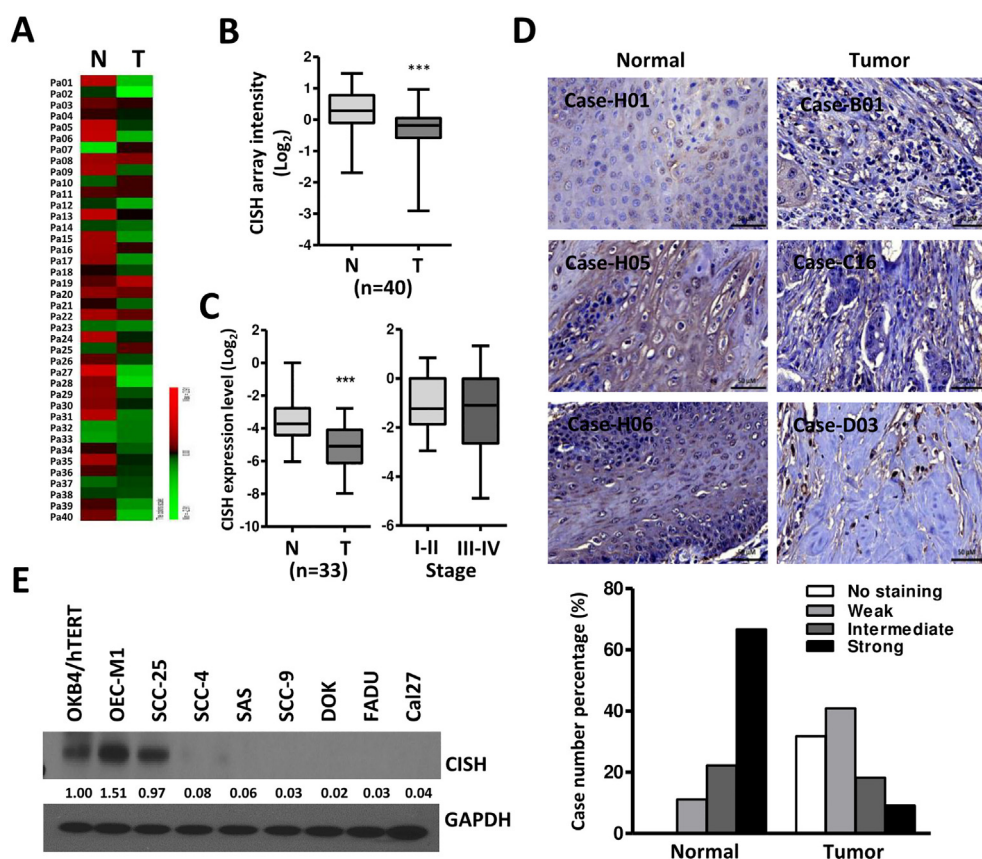


Fig. 1. CISH is downregulated in human OSCC. (A) Heat map of CISH expression in 40 OSCC tissue pairs (GSE37991). Red, overexpression; green, downexpression. (B) Array intensity of CISH in 40 of OSCC tumors compared with their own adjacent normal tissues. CISH intensity is expressed as the log₂ ratios. Data are represented as mean \pm SD; ***, $p < 0.001$. (C) Validation of CISH expression by qRT-PCR in 33 of OSCC tumors compared with their own adjacent normal tissues or compared with patients' stage. CISH expression levels are expressed as the log₂ ratios. Data are represented as mean \pm SD; ***, $p < 0.001$. (D) Immunohistochemical analysis of CISH in oral cancer tissue array. Bars in the right lower corners of all photos are equivalent to 50 μ m. Bar charts show the percentage of CISH staining score for the oral specimens in the tissue array, including 9 cases of normal tissue and 22 cases of OSCC. The CISH staining intensity was scored as follows: No staining, Weak, Intermediate and Strong. (E) Western blotting analysis of CISH expression in total cell lysates of the human OSCC cell lines. OKB4/hTERT was an hTERT gene transformed keratinocyte and used as the normal control. Glyceraldehyde-3-phosphate dehydrogenase (GAPDH) was used as an internal control. Numerical values for protein band intensities are shown below the gels. The values were quantitated by densitometry and normalized to GAPDH.

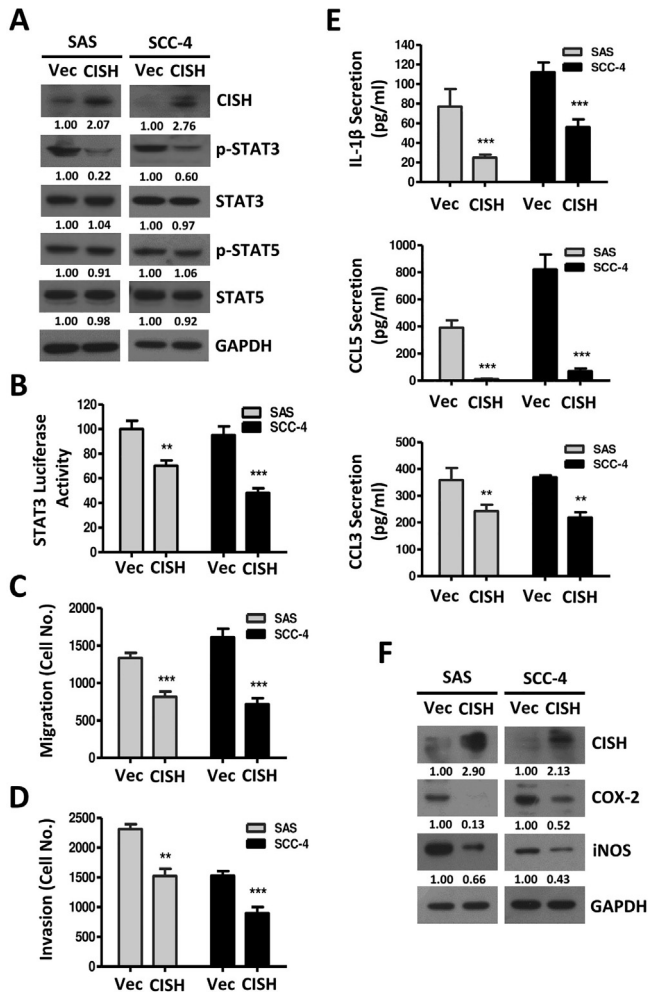


Fig. 2. Phenotypic effects of dysregulated CISH in OSCC cell lines. (A) Western blot analysis of the STAT3, 5 and their phosphorylation form after transfection of control vector (Vec) or CISH expression vector (CISH) for 48 h in SAS and SCC-4 cells. GAPDH was used as protein loading control. Numerical values for protein band intensities are shown below the gels. The values were quantitated by densitometry and normalized to GAPDH. (B) The effect of CISH on the transcriptional activity of the construct containing the STAT3 binding sequence. The relative luciferase activities are the ratios of Renilla luciferase normalized to the vector alone control. (C) Migration assay following CISH overexpression for 24 h using Matrigel non-coated Boyden chamber assay in SAS and SCC-4 cells. (D) Invasion assay following CISH overexpression for 24 h using Matrigel coated Boyden chamber assay in SAS and SCC-4 cells. (E) CCL3, CCL5 and IL-1 β levels in cultured medium of CISH overexpression SAS and SCC-4 cells measured by ELISA (compared with Vec control). (F) Western blot analysis of the CISH, COX-2 and iNOS after transfection of CISH for 48 h in SAS and SCC-4 cells. GAPDH was used as protein loading control. All data are represented as mean \pm SD; **, $p < 0.01$; ***, $p < 0.001$.

the migration (Fig. 4D) and invasion (Fig. 4E) activities induced by miR-944 overexpression. Similar results were obtained in pro-inflammation molecules secretion and transwell assay with another OSCC cell lines SCC-25 (Fig. S3B and Fig. S4A-C). These data demonstrate that miR-944-mediated CISH functions are crucial in regulating STAT3 activity, pro-inflammation molecules secretion, migration and invasive potential in OSCC cells.

MiR-944 are elevated in OSCC cells exposed to NNK

The results described above indicate that the dysregulation of miR-944 has a deep impact on multiple functions in OSCC tumorigenesis; however, the molecular mechanism of miR-944 regulation remain unclear. Recent evidence indicates that exposure to cigarette smoke causes numerous diseases, including cancer and inflammation [46]. Moreover, cigarette smoke exposure increases phosphorylation of STAT3 in several types of cancers and head and neck cancer cells [40,47,48]. Because of 4-(Methyl nitrosamino)-1-(3-pyridyl)-1-butanone (NNK) is one of the major components of cigarette smoke and effective carcinogen [49]. Therefore, we hypothesize that tobacco extract, such as NNK, may contribute to the miR-944 induction and the activation of STAT3 in OSCC. To test this hypothesis, we examined the effect of NNK on miR-944 expression in OEC-M1 and SCC-25 cells. We found that NNK significantly induced miR-944 expression in a time- and concentration-dependent manner (Fig. 5A, B). Then we determined whether CISH mRNA was targeted by NNK-induced miR-944. NNK treatment significantly suppressed the luciferase reporter activity of the wild-type CISH 3'-UTR, but did not affect the mutant CISH 3'-UTR (Fig. 5C). To determine whether miR-944 is required for NNK-induced STAT3 activation in OSCC cells, we transfected with the miR-944 inhibitor (AM) in OEC-M1 and SCC-25 cells. We found that miR-944 inhibitor (AM) significantly repressed the NNK-induced miR-944 expression (Fig. 5D). Furthermore, miR-944 inhibitor (AM) not only restored the CISH protein levels that suppressed by NNK treatment but also decreased the NNK-induced STAT3 phosphorylation (Fig. 5E). To confirm this finding, the effect of NNK on the STAT3-mediated pro-inflammation genes expression were determined. Transfection of cells with miR-944 inhibitor (AM) essentially inhibited the NNK-induced pro-inflammation genes expression (COX-2 and iNOS) (Fig. 6A) and pro-inflammation cytokines secretion (CCL3, CCL5 and IL-1 β) (Fig. 6B). In addition, the miR-944 inhibitor (AM) also attenuated the migration and invasion activities (Fig. 6C) induced by NNK treatment.

MiR-944 is located in the intron 4 of tumor protein p63 (*TP63*) gene and maps to chromosome 3q27-28 [50,51]. Many studies have reported that intronic miRNAs that are co-expressed with their host genes and play important roles [52,53]. Here, we measured the expressions of TP63 in OSCC cells exposed to NNK. We found that NNK significantly induced TP63 expression in OEC-M1 and SCC-25 cells (Fig. 6D). Furthermore, the expression of miR-944 was significantly correlated with the expression of TP63 ($r = 0.41$, $p = 0.0178$) in OSCC specimens ($n = 33$), indicating that that miR-944 is likely co-expressed with its host gene *TP63* (Fig. 6E).

Discussion

The importance of inflammation-associated tumorigenesis has received increasing attention in recent years. Abundant evidence suggests a crucial role for STAT3 in inducing oncogenic inflammatory conditions, both at the initiation of malignant transformation and during cancer progression [54,55]. For cancer inflammation, STAT3 signaling is a major intrinsic pathway because it is frequently activated in cancer cells and capable of inducing a large number of genes encoding for inflammation [6]. STAT3 hyperactivation may be due to two molecular events, one is constitutive activation by cytokine stimulation and the other is loss of SOCS proteins expression [16,56]. Herein, we uncover that STAT3 can be activated through a miR-944-mediated CISH down-expression pattern. Furthermore, our results clearly demonstrated that NNK-induced TP63/miR-944 co-expression plays an important role in oral carcinogenesis. This is the first investigation to provide mechanistic data linking miR-944/CISH/STAT3-mediated inflammation to tumorigenesis.

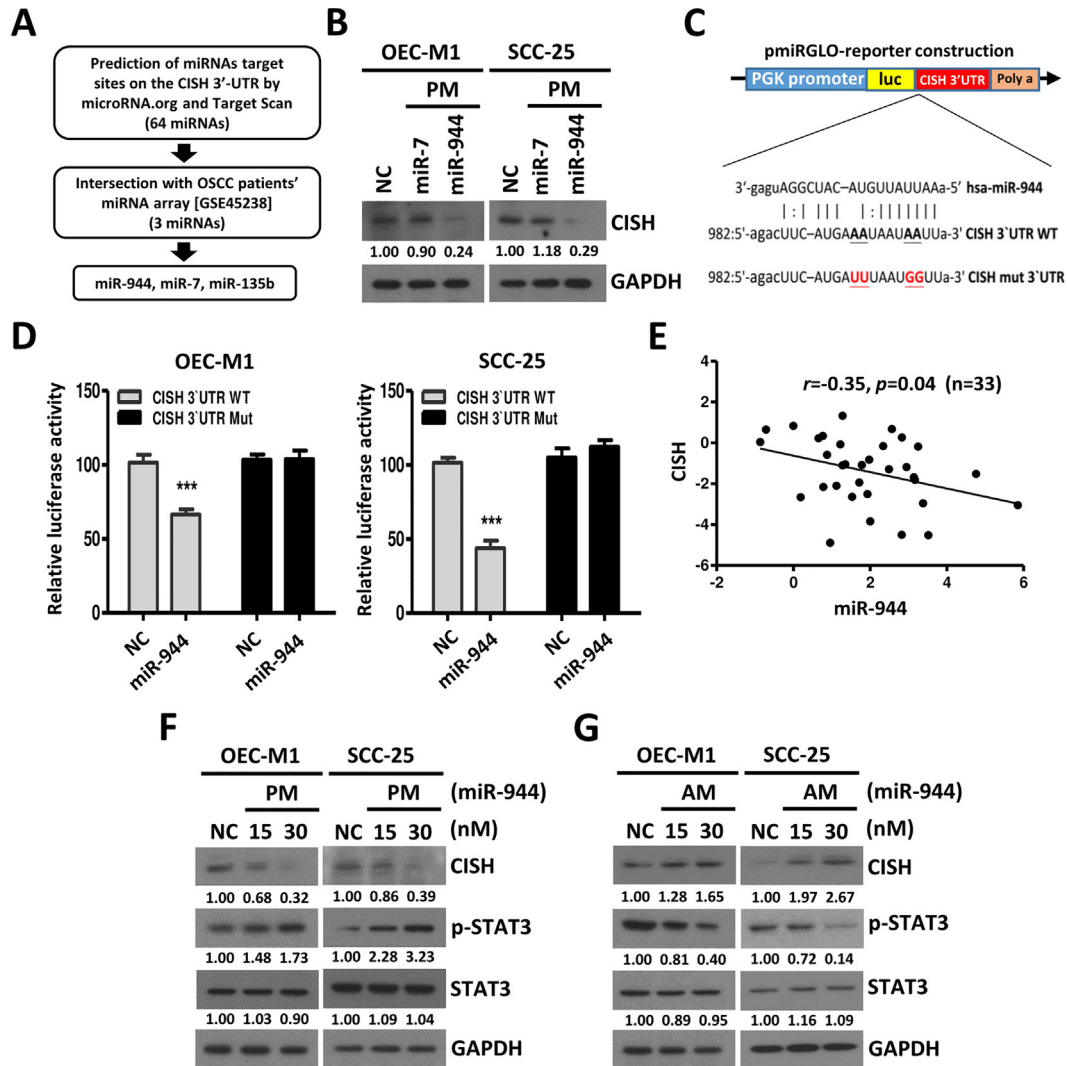


Fig. 3. CISH is a direct target of miR-944. (A) Flow chart of predicted miRNA which targets CISH 3'-UTR using two independent algorithms (microRNA.org and TargetScan) combined with our patients' miRNA array data (GSE45238). (B) Western blot analysis of CISH protein after transfection of miR-944 mimics (PM) with 30 nM for 48 h in OEC-M1 and SCC-25 cells. (C) Schematic representation of the putative miR-944 binding sequence in the 3'-UTR of CISH with wild-type form (CISH 3'UTR WT) and mutant form (CISH 3'UTR Mut). The mutated nucleotides are labeled with underline. (D) Luciferase activity assays were performed after OEC-M1 and SCC-25 cells transfected with luciferase vectors containing the wide-type or mutant CISH 3'-UTR, in response to miR-944 over-expression. The relative luciferase activity of each sample is measured at 48 h after transfection and normalized to Renilla luciferase activity. (E) Correlation analysis of miR-944 and CISH in human OSCC patients ($n = 33$) by qRT-PCR analysis. Western blot analysis of the CISH, STAT3 and phosphor-STAT3 after transfection of miR-944 mimics (PM) (F) or miR-944 inhibitors (AM) (G) with indicated concentration for 48 h in OEC-M1 and SCC-25 cells. All data are presented as mean \pm SD; ***, $p < 0.001$ versus scramble control (NC). GAPDH was used as protein loading control. Numerical values for protein band intensities are shown below the gels. The values were quantitated by densitometry and normalized to GAPDH.

CISH is known to function as a negative feedback regulator of the signaling pathway induced by specific cytokines and growth factors [13,57]. CISH has been reported to associate with the interleukin 2 (IL-2) receptor β -chain to disrupt the IL-2-induced Jak-STAT5 activity [58,59]. In addition, CISH was substantially induced by IL-4, negatively regulated the activation of STAT3, STAT5 and STAT6 in T cells. CISH-deficient mice could enhance the phosphorylation of STAT3, STAT5 and STAT6, and subsequently developed a lung disorder that resembled allergic airway inflammation [60]. Recently, CISH was demonstrated to mediate the eosinophilic inflammation by regulating IL-13-induced CCL26 production [61]. These findings suggest that CISH plays a key role in the inflammation in many diseases. However, the roles of CISH in oral cancer inflam-

mation remain unclear. In this study, we found that CISH down-expression enhanced STAT3 phosphorylation but not that of STAT5 in oral cancer. The persistent activation of STAT3 not only promotes tumor cell migration and invasion, but also induces a large number of pro-inflammatory genes expression and secretion, including CCL3, CCL5, IL-1 β , COX-2 and iNOS. We believe that these pro-inflammatory mediators are required for inducing and maintaining a pro-carcinogenic condition in tumor microenvironment. For example, CCL3 has been reported to promote vascular endothelial growth factor-A (VEGF-A) expression and angiogenesis in human osteosarcoma cells [62]. And CCL3-deficient mice were significantly protected from carcinogen-induced hepatocellular carcinoma progression *in vivo* [63]. An interaction between CCL5 and its

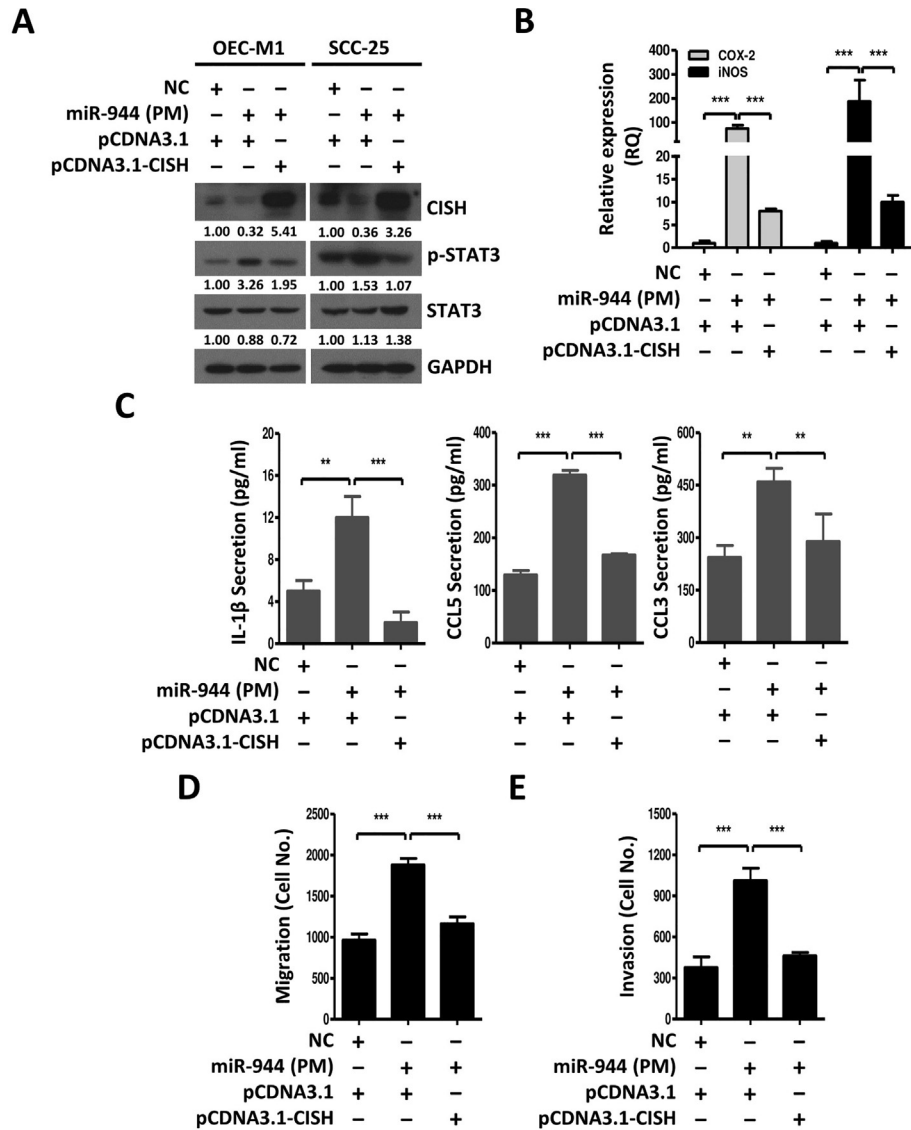


Fig. 4. miR-944 regulates OSCC cell functions through targeting CISH. OSCC cells were transfected with miR-944 mimics (PM) or scramble control (NC) for 24 h and then transfected with CISH expression vector without 3'-UTR (pCDNA3.1-CISH) or control vector (pCDNA3.1) for another 24 h. Under this condition, the level of CISH, STAT3 and phosphor-STAT3 were determined in OEC-M1 and SCC-25 cells by western blotting (A). The RNA level of COX-2 and iNOS (B), protein level of CCL3, CCL5 and IL-1β levels in cultured medium (C), migration ability (D), and invasion ability (E) were measured by qRT-PCR, ELISA and transwell assays in OEC-M1 cells. All data are presented as mean ± SD; **, $p < 0.01$; ***, $p < 0.001$ versus scramble control (NC). GAPDH was used as protein loading control. Numerical values for protein band intensities are shown below the gels. The values were quantitated by densitometry and normalized to GAPDH.

receptors C-C chemokine receptor type 5 (CCR5) may favor tumor development in multiple ways, such as stimulating angiogenesis, promoting the release of matrix metalloproteases, inducing the recruitment of tumor-associated macrophage (TAM) into the tumor microenvironment, and taking part in immune evasion mechanisms [64,65]. In addition, IL-1β is also a multifunctional and pro-inflammatory cytokine released to the tumor microenvironment, and involved in the process of tumor growth and metastasis. Chen's group recently described that IL-1β is able to regulate the epithelial-to-mesenchymal transition (EMT) by activating Twist to promote cancer proliferation and migration [66]. Recently, it has been reported that numerous tumors overexpress COX-2 and iNOS, which both contribute to T-cell dysfunction in the tumor microenvironment [67]. COX2 and its metabolite prostaglandin E2 (PGE2) could induce the accumulation of myeloid-derived suppressor cells (MDSCs), which

inhibit the activation of CD4⁺ and CD8⁺ T cells and contribute to tumor immune evasion [68]. Likewise, tumor cells exhibit high level of iNOS may also recruit MDSCs into the tumor microenvironment to induce cell cycle arrest of T cells, and then promote tumor progression and angiogenesis [69]. Thus, the use of inhibitors against COX-2 and iNOS may stimulate cellular immunity and block tumor growth [67,70]. Taken together, these findings indicates that STAT3-driven pro-inflammatory genes expression from tumor cells plays an important role in regulating of cancer-associated inflammation microenvironment. Moreover, CISH deficiency could induce the activation of STAT3 in oral cancer. Thus the investigation of mechanisms of CISH deficiency in oral carcinogenesis is imperative and of great significance.

In this study, we demonstrated that miR-944 is upregulated in oral cancer tissues and promotes tumor migration and invasion, suggesting that

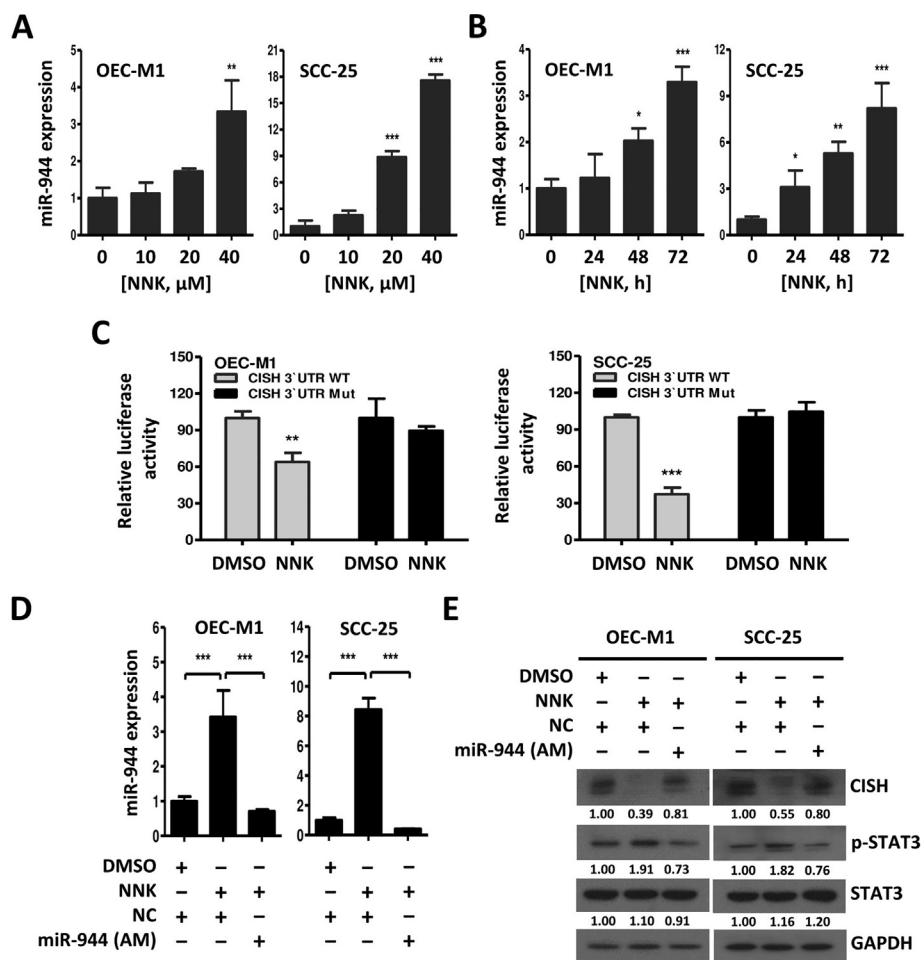


Fig. 5. NNK exposure induces miR-944 expression. (A) OEC-M1 and SCC-25 cells were treated with NNK (10–40 μM) for 72 h, and the miR-944 expression level was measured by qRT-PCR analysis. (B) OEC-M1 and SCC-25 cells were treated with 20 μM of NNK for indicated time (24–72 h), and the miR-944 expression level was measured by qRT-PCR analysis. (C) Luciferase activity assays were performed after OEC-M1 and SCC-25 cells transfected with luciferase vectors containing the wide-type or mutant CISH 3'-UTR, in response to DMSO control or 20 μM of NNK treatment. The relative luciferase activity of each sample is measured at 72 h after transfection and normalized to Renilla luciferase activity. OEC-M1 and SCC-25 cells were transfected with miR-944 inhibitors (AM) for 12 h, and followed by 20 μM of NNK treatment for another 72 h. Under this condition, the expression level of miR-944 was determined by qRT-PCR analysis (D), and the protein level of CISH, STAT3, phosphor-STAT3 and GAPDH were determined by western blot analysis (E). All data are presented as mean \pm SD; *, $p < 0.05$; **, $p < 0.01$; ***, $p < 0.001$. Numerical values for protein band intensities are shown below the gels. The values were quantitated by densitometry and normalized to GAPDH.

miR-944 may function as an oncogene in oral cancer. To date, several targets of miR-944 have been reported. For example, one recent study showed that miR-944 is significantly overexpressed in cervical cancer and promotes cell proliferation, migration, and invasion by targeting HECT domain ligase W2 (HECW2) and S100P binding protein (S100BP) [71]. He et al. showed that miR-944 is significantly overexpressed in breast cancer and promotes the chemotherapy resistance of breast cancer by targeting BCL2 interacting protein 3 (BNIP3) [72]. On the contrary, it has been demonstrated that miR-944 repressed cell proliferation, migration and invasion by targeting GATA binding protein 6 (GATA6) in colorectal cancer [73]. Thus, whether miR-944 serves as oncogene or suppressor is depending on the different tumor type. Here, we identified CISH as a novel target for miR-944 in oral cancer that was not reported previously to our knowledge. CISH expression is significantly reduced in miR-944 overexpressed oral cancer cells. The mechanistic data also suggest that miR-944-mediated CISH silencing then promote pro-inflammatory genes expression and secretion by activating STAT3 activity. Therefore, it is conceivable that the miR-944/CISH/STAT3 axis

is critical for maintaining a pro-carcinogenic microenvironment in oral cancer and may potentially serve as a therapeutic target.

Recently, there has been a growing evidence showing that miRNAs play a role in the cigarette smoking-related inflammatory process [74]. Cigarette smoking has been implicated to correlate with STAT3 activation in oral carcinogenesis [36], but the molecular mechanisms by which cigarette smoke products activate STAT3 in oral cancer remain to be established. Notably, our subsequent experiments demonstrated that NNK can elevate the level of miR-944 and knockdown of miR-944 attenuates NNK-induced STAT3 phosphorylation, as well as production of CCL3, CCL5, IL-1 β , COX-2 and iNOS, by targeting CISH, indicating a role of miR-944 in the cigarette smoking-induced inflammation. Interestingly, miR-944 is located in the intron of its host gene (*TP63*) and mapped to human 3q27-28, a region frequently amplified in cancer [75]. It has been reported that *TP63* amplification and TP63 overexpression are prevalent in squamous carcinomas and participate in tumor progression [76]. As showed in this study, NNK treatment induced both TP63 and miR-944 expression. Furthermore, the expression of miR-944 was significantly

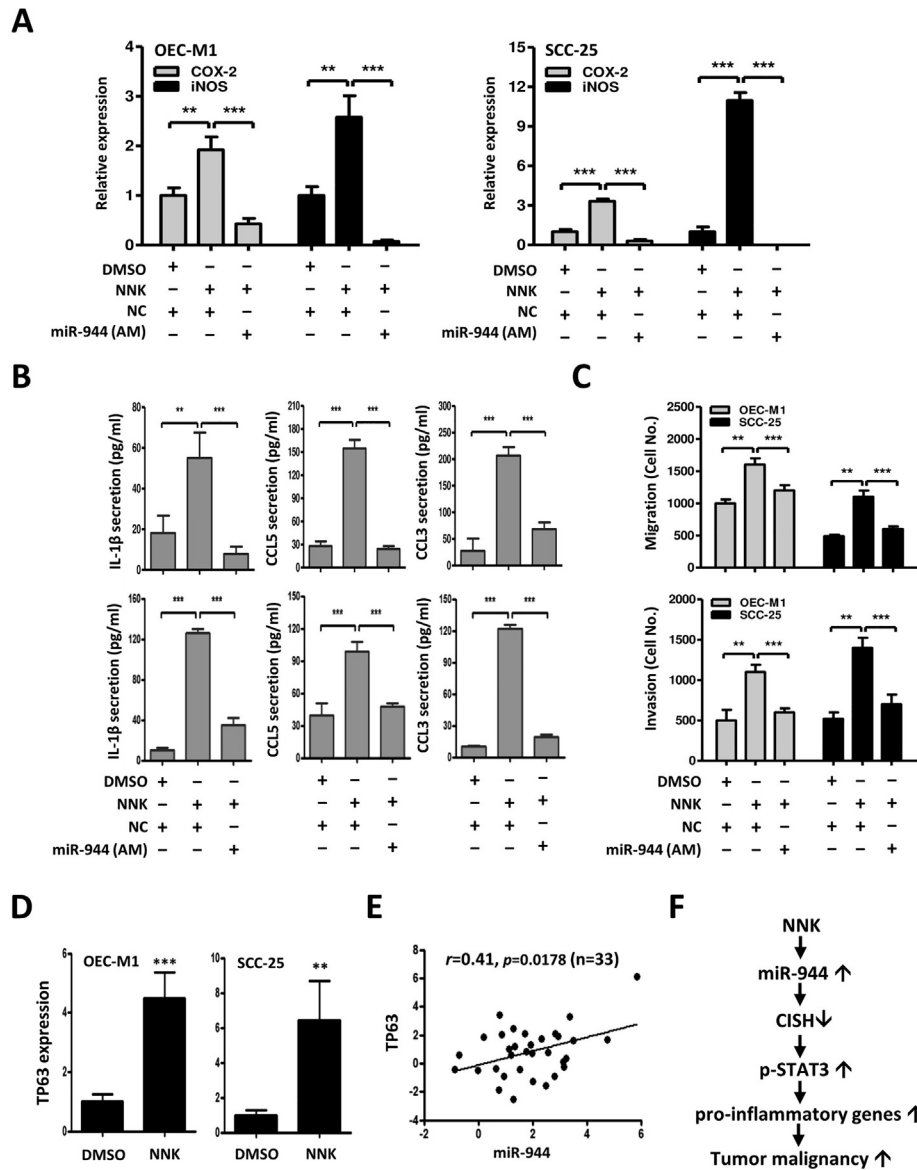


Fig. 6. The effects of NNK on the STAT3-mediated pro-inflammation genes. OEC-M1 and SCC-25 cells were transfected with miR-944 inhibitors (AM) for 12 h, and followed by 20 μM of NNK treatment for another 72 h. The RNA level of COX-2 and iNOS in cells (A), protein level of CCL3, CCL5 and IL-1β in cultured medium (B) were measured by qRT-PCR or ELISA. (C) Migration and invasion ability were measured by transwell assays in OEC-M1 and SCC-25 cells. (D) OEC-M1 and SCC-25 cells were treated with 20 μM of NNK for 72 h, and the TP63 expression level was measured by qRT-PCR analysis. (E) Correlation analysis of miR-944 and TP63 in human OSCC patients (n = 33) by qRT-PCR analysis. (F) Proposed model for comprehensive NNK-induced upregulation of miR-944 in stimulating STAT3 activation and pro-inflammatory genes expression through suppression of CISH. All data are represented as mean ± SD; **, $p < 0.01$; ***, $p < 0.001$.

correlated with the expression of TP63 in OSCC specimens, suggesting that miR-944 is co-expressed with its host gene *TP63* and plays an important role in oral carcinogenesis. Although the mechanisms involved in cigarette smoking-induced TP63/miR-944 expression are poorly understood. A link from inflammation to malignant transformation through miR-944 has been established. Such information contributes to an understanding of how oral cancer is caused by cigarette smoking.

In summary, we have provided evidence that exposure of cells to NNK induces an inflammatory response that contributes to NNK-induced malignant transformation. We have shown that the NNK-induced upregulation of miR-944 in stimulating STAT3 activation and pro-inflammatory genes expression through suppression of CISH (Fig. 6F). These results highlight a relevant link, through miR-944/CISH/STAT3 axis, between cigarette smoking to inflammatory microenvironment,

which contributes a possible mechanism for cigarette smoking-induced oral carcinogenesis.

Declaration of Competing Interest

The authors declare that they have no known competing financial interests or personal relationships that could have appeared to influence the work reported in this paper.

Acknowledgements

The authors are grateful for support with the clinical samples from the Tissue Bank, Research Center of Clinical Medicine, National Cheng Kung

University Hospital. We also thank the pathology core laboratory which is funded by the National Health Research Institutes (NHRI) of Taiwan for technical support in immunohistochemistry experiment for optical image capture.

Funding

This work was supported by National Health Research Institutes (NHRI) grants from Taiwan (NHRI-CA107-PP03, NHRI-CA108-PP03), and the Ministry of Health and Welfare (MOHW) grants from Taiwan (MOHW 108-TDU-B-212-124026, MOHW 109-TDU-B-212-134013).

Authors' contributions

HYP and SGS conceived and designed the experiments. HYP, YSS and SGS performed the data analysis and interpretation. HYP, YMH, GHW and STC performed the experiments. JRH and YSS contributed materials. HYP and SGS were involved in the manuscript preparation. SGS contributed in the coordination of the study. All authors read and approved the final manuscript.

Appendix A. Supplementary data

Supplementary data to this article can be found online at <https://doi.org/10.1016/j.neo.2020.08.005>.

References

- Warnakulasuriya S. Global epidemiology of oral and oropharyngeal cancer. *Oral Oncol* 2009;**45**:309–16.
- Ord RA, Blanchaert Jr RH. Current management of oral cancer. A multidisciplinary approach. *J Am Dent Assoc* 2001;**132** Suppl:19S–23S.
- Zain RB. Cultural and dietary risk factors of oral cancer and precancer—a brief overview. *Oral Oncol* 2001;**37**:205–10.
- Jerjes W, Upile T, Petrie A, Riskalla A, Hamdoon Z, Vourvachis M, et al. Clinicopathological parameters, recurrence, locoregional and distant metastasis in 115 T1–T2 oral squamous cell carcinoma patients. *Head Neck Oncol* 2010;**2**:9.
- Wang L, Yi T, Zhang W, Pardoll DM, Yu H. IL-17 enhances tumor development in carcinogen-induced skin cancer. *Cancer Res* 2010;**70**:10112–20.
- Yu H, Pardoll D, Jove R. STATs in cancer inflammation and immunity: a leading role for STAT3. *Nat Rev Cancer* 2009;**9**:798–809.
- Mantovani A, Allavena P, Sica A, Balkwill F. Cancer-related inflammation. *Nature* 2008;**454**:436–44.
- Kortylewski M, Xin H, Kujawski M, Lee H, Liu Y, Harris T, et al. Regulation of the IL-23 and IL-12 balance by Stat3 signaling in the tumor microenvironment. *Cancer Cell* 2009;**15**:114–23.
- Hideshima T, Nakamura N, Chauhan D, Anderson KC. Biologic sequelae of interleukin-6 induced PI3-K/Akt signaling in multiple myeloma. *Oncogene* 2001;**20**:5991–6000.
- Balkwill F, Charles KA, Mantovani A. Smoldering and polarized inflammation in the initiation and promotion of malignant disease. *Cancer Cell* 2005;**7**:211–7.
- Jarnicki A, Putoczki T, Ernst M. Stat3: linking inflammation to epithelial cancer - more than a "gut" feeling? *Cell Div* 2010;**5**:14.
- Bromberg J. Stat proteins and oncogenesis. *J Clin Invest* 2002;**109**:1139–42.
- Yasukawa H, Sasaki A, Yoshimura A. Negative regulation of cytokine signaling pathways. *Annu Rev Immunol* 2000;**18**:143–64.
- Tamiya T, Kashiwagi I, Takahashi R, Yasukawa H, Yoshimura A. Suppressors of cytokine signaling (SOCS) proteins and JAK/STAT pathways: regulation of T-cell inflammation by SOCS1 and SOCS3. *Arterioscler Thromb Vasc Biol* 2011;**31**:980–5.
- Yoshimura A, Suzuki M, Sakaguchi R, Hanada T, Yasukawa H. SOCS, inflammation, and autoimmunity. *Front Immunol* 2012;**3**:20.
- Inagaki-Ohara K, Kondo T, Ito M, Yoshimura A. SOCS, inflammation, and cancer. *JAKSTAT* 2013;**2** e24053.
- Jiang M, Zhang WW, Liu P, Yu W, Liu T, Yu J. Dysregulation of SOCS-mediated negative feedback of cytokine signaling in carcinogenesis and its significance in cancer treatment. *Front Immunol* 2017;**8**:70.
- Melzner I, Weniger MA, Bucur AJ, Bruderlein S, Dorsch K, Hasel C, et al. Biallelic deletion within 16p13.13 including SOCS-1 in Karpas1106P mediastinal B-cell lymphoma line is associated with delayed degradation of JAK2 protein. *Int J Cancer* 2006;**118**:1941–4.
- Franke S, Wlodarska I, Maes B, Vandenbergh P, Delabie J, Hagemeijer A, et al. Lymphocyte predominance Hodgkin disease is characterized by recurrent genomic imbalances. *Blood* 2001;**97**:1845–53.
- Weniger MA, Melzner I, Menz CK, Wegener S, Bucur AJ, Dorsch K, et al. Mutations of the tumor suppressor gene SOCS-1 in classical Hodgkin lymphoma are frequent and associated with nuclear phospho-STAT5 accumulation. *Oncogene* 2006;**25**:2679–84.
- Guillem V, Amat P, Cervantes F, Alvarez-Larran A, Cervera J, Maffioli M, et al. Functional polymorphisms in SOCS1 and PTPN22 genes correlate with the response to imatinib treatment in newly diagnosed chronic-phase chronic myeloid leukemia. *Leuk Res* 2012;**36**:174–81.
- Butterbach K, Beckmann L, de Sanjose S, Benavente Y, Becker N, Foretova L, et al. Association of JAK-STAT pathway related genes with lymphoma risk: results of a European case-control study (EpiLymph). *Br J Haematol* 2011;**153**:318–33.
- Sutherland KD, Lindeman GJ, Choong DYH, Wittlin S, Brentzell L, Phillips W, et al. Differential hypermethylation of SOCS genes in ovarian and breast carcinomas. *Oncogene* 2004;**23**:7726–33.
- Isomoto H. Epigenetic alterations in cholangiocarcinoma-sustained IL-6/STAT3 signaling in cholangio- carcinoma due to SOCS3 epigenetic silencing. *Digestion* 2009;**79**(Suppl 1):2–8.
- Hatimaz O, Ure U, Ar C, Akyerli C, Soysal T, Ferhanoglu B, et al. The SOCS-1 gene methylation in chronic myeloid leukemia patients. *Am J Hematol* 2007;**82**:729–30.
- Gao SM, Chen CQ, Wang LY, Hong LL, Wu JB, Dong PH, et al. Histone deacetylases inhibitor sodium butyrate inhibits JAK2/STAT signaling through upregulation of SOCS1 and SOCS3 mediated by HDAC8 inhibition in myeloproliferative neoplasms. *Exp Hematol* 2013;**41**, 261-70 e4.
- Xiong H, Du W, Zhang YJ, Hong J, Su WY, Tang JT, et al. Trichostatin A, a histone deacetylase inhibitor, suppresses JAK2/STAT3 signaling via inducing the promoter-associated histone acetylation of SOCS1 and SOCS3 in human colorectal cancer cells. *Mol Carcinog* 2012;**51**:174–84.
- Bartel DP. MicroRNAs: genomics, biogenesis, mechanism, and function. *Cell* 2004;**116**:281–97.
- Wu T, Xie M, Wang X, Jiang X, Li J, Huang H. miR-155 modulates TNF- α -inhibited osteogenic differentiation by targeting SOCS1 expression. *Bone* 2012;**51**:498–505.
- Ye J, Guo R, Shi Y, Qi F, Guo C, Yang L. miR-155 regulated inflammation response by the SOCS1-STAT3-PDCD4 axis in atherosclerosis. *Mediators Inflamm* 2016;**2016**:8060182.
- Collins AS, McCoy CE, Lloyd AT, O'Farrelly C, Stevenson NJ. miR-19a: an effective regulator of SOCS3 and enhancer of JAK-STAT signalling. *PLoS one* 2013;**8** e69090.
- Das R, Gregory PA, Fernandes RC, Denis I, Wang Q, Townley SL, et al. MicroRNA-194 promotes prostate cancer metastasis by inhibiting SOCS2. *Cancer Res* 2017;**77**:1021–34.
- Peng HY, Jiang SS, Hsiao JR, Hsiao M, Hsu YM, Wu GH, et al. IL-8 induces miR-424-5p expression and modulates SOCS2/STAT5 signaling pathway in oral squamous cell carcinoma. *Mol Oncol* 2016;**10**:895–909.
- Kneitz B, Krebs M, Kalogirou C, Schubert M, Joniau S, van Poppel H, et al. Survival in patients with high-risk prostate cancer is predicted by miR-221, which regulates proliferation, apoptosis, and invasion of prostate cancer cells by inhibiting IRF2 and SOCS3. *Cancer Res* 2014;**74**:2591–603.
- Ru P, Steele R, Hsueh EC, Ray RB. Anti-miR-203 upregulates SOCS3 expression in breast cancer cells and enhances cisplatin chemosensitivity. *Genes Cancer* 2011;**2**:720–7.
- Nagpal JK, Mishra R, Das BR. Activation of Stat-3 as one of the early events in tobacco chewing-mediated oral carcinogenesis. *Cancer* 2002;**94**:2393–400.
- Geraghty P, Wyman AE, Garcia-Arcos I, Dabo AJ, Gadhvi S, Foronjy R. STAT3 modulates cigarette smoke-induced inflammation and protease expression. *Front Physiol* 2013;**4**:267.

38. Sano S, Chan KS, Kira M, Kataoka K, Takagi S, Tarutani M, et al. Signal transducer and activator of transcription 3 is a key regulator of keratinocyte survival and proliferation following UV irradiation. *Cancer Res* 2005;**65**:5720–9.
39. Bronte-Tinkew DM, Terebiznik M, Franco A, Ang M, Ahn D, Mimuro H, et al. Helicobacter pylori cytotoxin-associated gene A activates the signal transducer and activator of transcription 3 pathway in vitro and in vivo. *Cancer Res* 2009;**69**:632–9.
40. Liu X. STAT3 activation inhibits human bronchial epithelial cell apoptosis in response to cigarette smoke exposure. *Biochem Biophys Res Commun* 2007;**353**:121–6.
41. Zhao Y, Xu Y, Li Y, Xu W, Luo F, Wang B, et al. NF-kappaB-mediated inflammation leading to EMT via miR-200c is involved in cell transformation induced by cigarette smoke extract. *Toxicol Sci* 2013;**135**:265–76.
42. Masuda M, Wakasaki T, Suzui M, Toh S, Joe AK, Weinstein IB. Stat3 orchestrates tumor development and progression: the Achilles' heel of head and neck cancers? *Curr Cancer Drug Targets* 2010;**10**:117–26.
43. Su WP, Lo YC, Yan JJ, Liao IC, Tsai PJ, Wang HC, et al. Mitochondrial uncoupling protein 2 regulates the effects of paclitaxel on Stat3 activation and cellular survival in lung cancer cells. *Carcinogenesis* 2012;**33**:2065–75.
44. Wang SW, Sun YM. The IL-6/JAK/STAT3 pathway: potential therapeutic strategies in treating colorectal cancer (Review). *Int J Oncol* 2014;**44**:1032–40.
45. Shiah SG, Hsiao JR, Chang WM, Chen YW, Jin YT, Wong TY, et al. Downregulated miR329 and miR410 promote the proliferation and invasion of oral squamous cell carcinoma by targeting Wnt-7b. *Cancer Res* 2014;**74**:7560–72.
46. Hamilton G, Rath B. Smoking, inflammation and small cell lung cancer: recent developments. *Wien Med Wochenschr* 2015;**165**:379–86.
47. Macha MA, Matta A, Chauhan SS, Siu KW, Ralhan R. Guggulsterone (GS) inhibits smokeless tobacco and nicotine-induced NF-kappaB and STAT3 pathways in head and neck cancer cells. *Carcinogenesis* 2011;**32**:368–80.
48. Chen RJ, Ho YS, Guo HR, Wang YJ. Rapid activation of Stat3 and ERK1/2 by nicotine modulates cell proliferation in human bladder cancer cells. *Toxicol Sci* 2008;**104**:283–93.
49. Hecht SS. Tobacco carcinogens, their biomarkers and tobacco-induced cancer. *Nat Rev Cancer* 2003;**3**:733–44.
50. Witten D, Tibshirani R, Gu SG, Fire A, Lui WO. Ultra-high throughput sequencing-based small RNA discovery and discrete statistical biomarker analysis in a collection of cervical tumours and matched controls. *BMC Biol* 2010;**8**:58.
51. Heselmeyer K, Schrock E, du Manoir S, Blegen H, Shah K, Steinbeck R, et al. Gain of chromosome 3q defines the transition from severe dysplasia to invasive carcinoma of the uterine cervix. *PNAS* 1996;**93**:479–84.
52. Ramirez CM, Goedeke L, Rotllan N, Yoon JH, Cirera-Salinas D, Mattison JA, et al. MicroRNA 33 regulates glucose metabolism. *Mol Cell Biol* 2013;**33**:891–902.
53. Sowa N, Horie T, Kuwabara Y, Baba O, Watanabe S, Nishi H, et al. MicroRNA 26b encoded by the intron of small CTD phosphatase (SCP) 1 has an antagonistic effect on its host gene. *J Cell Biochem* 2012;**113**:3455–65.
54. Aggarwal BB, Kunnumakkara AB, Harikumar KB, Gupta SR, Tharakan ST, Koca C, et al. Signal transducer and activator of transcription-3, inflammation, and cancer: how intimate is the relationship? *Ann N Y Acad Sci* 2009;**1171**:59–76.
55. Bromberg J, Wang TC. Inflammation and cancer: IL-6 and STAT3 complete the link. *Cancer Cell* 2009;**15**:79–80.
56. Sasi W, Sharma AK, Mokbel K. The role of suppressors of cytokine signalling in human neoplasms. *Mol Biol Int* 2014;**2014** 630797.
57. Trengove MC, Ward AC. SOCS proteins in development and disease. *Am J Clin Exp Immunol* 2013;**2**:1–29.
58. Matsumoto A, Masuhara M, Mitsui K, Yokouchi M, Ohtsubo M, Misawa H, et al. CIS, a cytokine inducible SH2 protein, is a target of the JAK-STAT5 pathway and modulates STAT5 activation. *Blood* 1997;**89**:3148–54.
59. Aman MJ, Migone TS, Sasaki A, Ascherman DP, Zhu M, Soldaini E, et al. CIS associates with the interleukin-2 receptor beta chain and inhibits interleukin-2-dependent signaling. *J Biol Chem* 1999;**274**:30266–72.
60. Yang XO, Zhang H, Kim BS, Niu X, Peng J, Chen Y, et al. The signaling suppressor CIS controls proallergic T cell development and allergic airway inflammation. *Nat Immunol* 2013;**14**:732–40.
61. Takeshima H, Horie M, Mikami Y, Makita K, Miyashita N, Matsuzaki H, et al. CISH is a negative regulator of IL-13-induced CCL26 production in lung fibroblasts. *Allergol Int* 2019;**68**:101–9.
62. Liao YY, Tsai HC, Chou PY, Wang SW, Chen HT, Lin YM, et al. CCL3 promotes angiogenesis by dysregulation of miR-374b/ VEGF-A axis in human osteosarcoma cells. *Oncotarget* 2016;**7**:4310–25.
63. Yang X, Lu P, Fujii C, Nakamoto Y, Gao JL, Kaneko S, et al. Essential contribution of a chemokine, CCL3, and its receptor, CCR1, to hepatocellular carcinoma progression. *Int J Cancer* 2006;**118**:1869–76.
64. Kershaw MH, Westwood JA, Darcy PK. Gene-engineered T cells for cancer therapy. *Nat Rev Cancer* 2013;**13**:525–41.
65. An G, Wu F, Huang S, Feng L, Bai J, Gu S, et al. Effects of CCL5 on the biological behavior of breast cancer and the mechanisms of its interaction with tumor-associated macrophages. *Oncol Rep* 2019;**42**:2499–511.
66. Guo R, Qin Y, Shi P, Xie J, Chou M, Chen Y. IL-1beta promotes proliferation and migration of gallbladder cancer cells via Twist activation. *Oncol Lett* 2016;**12**:4749–55.
67. Wu AA, Drake V, Huang HS, Chiu S, Zheng L. Reprogramming the tumor microenvironment: tumor-induced immunosuppressive factors paralyze T cells. *Oncimmunology* 2015;**4** e1016700.
68. Sinha P, Clements VK, Fulton AM, Ostrand-Rosenberg S. Prostaglandin E2 promotes tumor progression by inducing myeloid-derived suppressor cells. *Cancer Res* 2007;**267**:4507–13.
69. Kostourou V, Cartwright JE, Johnstone AP, Boulton JK, Cullis ER, Whitley G, et al. The role of tumour-derived iNOS in tumour progression and angiogenesis. *Br J Cancer* 2011;**104**:83–90.
70. Khan I, Al-Awadi FM, Thomas N, Haridas S, Anim JT. Cyclooxygenase-2 inhibition and experimental colitis: beneficial effects of phosphorothioated antisense oligonucleotide and meloxicam. *Scand J Gastroenterol* 2002;**37**:1428–36.
71. Xie H, Lee L, Scicluna P, Kavak E, Larsson C, Sandberg R, et al. Novel functions and targets of miR-944 in human cervical cancer cells. *Int J Cancer* 2015;**136**:E230–41.
72. He H, Tian W, Chen H, Jiang K. MiR-944 functions as a novel oncogene and regulates the chemoresistance in breast cancer. *Tumour Biol* 2016;**37**:1599–607.
73. Tang JT, Zhao J, Sheng W, Zhou JP, Dong Q, Dong M. Ectopic expression of miR-944 impairs colorectal cancer cell proliferation and invasion by targeting GATA binding protein 6. *J Cell Mol Med* 2019;**23**:3483–94.
74. Zong D, Liu X, Li J, Ouyang R, Chen P. The role of cigarette smoke-induced epigenetic alterations in inflammation. *Epigenet Chromatin* 2019;**12**:65.
75. Yang YC, Shyong WY, Chang MS, Chen YJ, Lin CH, Huang ZD, et al. Frequent gain of copy number on the long arm of chromosome 3 in human cervical adenocarcinoma. *Cancer Genet Cytogenet* 2001;**131**:48–53.
76. Massion PP, Taflan PM, Jamshedur Rahman SM, Yildiz P, Shyr Y, Edgerton ME, et al. Significance of p63 amplification and overexpression in lung cancer development and prognosis. *Cancer Res* 2003;**63**:7113–21.